The influence of stratum water composition on steel corrosion and the protective effect of the inhibitor in the presence of H_2S and CO_2

L.E. Tsygankova,[1]* R.K. Vagapov,[2] A.E. Abramov,[1] T.V. Semenyuk,[1] V.A. Igonina[1] and L.E. Isaeva[1]

[1]Derzhavin State University, ul. Internatsyonalnaya, 33, 392000 Tambov, Russian Federation
[2]Gazprom VNIIGAZ LLC, Proektiruemyi proezd 5537, 15, 1, Razvilka, s.p. Razvilkovskoe, Leninsky distr., 142717, Moscow Region, Russian Federation
**E-mail: vits21@mail.ru*

Abstract

Corrosion of St3 steel and protective effectiveness of an inhibitory composition (25–200 mg/l), which is a solution of nitrogen-containing compounds (polyamines) in a mixture of organic solvents, were studied in model stratum waters MW1 and MW2, differing in the degree of mineralization, saturated with H_2S and CO_2 and containing 0.25 mg/L CH_3COOH. Gravimetric methods have shown that the corrosion rate of steel in less mineralized MW1 environments is higher than in MW2 environments under static conditions both at room temperature and 80°C, and in stirred solutions in the presence of a hydrocarbon phase. The protective effectiveness of the inhibitory composition in the presence of H_2S in solution is higher in MW1, and in the presence of H_2S and CO_2, in contrast, in MW2 at room temperature and 80°C. The presence of H_2S and CO_2 in the solution contributes to a higher protective effectiveness of the inhibitory composition in both stratum waters ($Z = 90\%$) than in the presence of H_2S ($Z = 60–70\%$), both at room temperature and 80°C. Under dynamic conditions at 10% hydrocarbon phase content, its value exceeds 90%. The influence of acetic acid present in the solution is discussed. The impedance spectroscopy method made it possible to evaluate the adsorption of the components of the inhibitory composition. This made it possible to calculate the surface coverage with an inhibitor, to determine the type of adsorption isotherm, and to calculate the adsorption free energy.

Received: March 1, 2024. Published: March 14, 2024 doi: 10.17675/2305-6894-2024-13-1-29

Keywords: *steel, corrosion, formation water, hydrogen sulfide, carbon dioxide, protection, inhibitory composition, corrosion products.*

Introduction

Hydrogen sulfide and carbon dioxide corrosion in the oil and gas industry have been studied for a long time. Various methods have been proposed to reduce metal losses from these types of corrosion, among which the use of corrosion inhibitors is considered the most effective

and economical. Inhibitor protection is important to reduce the risk of corrosion damage to pipelines of the oil and gas complex [1, 2]. Numerous studies have been devoted to their application; a review of some of them is given in [3]. It is noted in [4] that the composition of stratum waters has a significant influence on the corrosion behavior of metal equipment. It is assumed that, in addition to H_2S and CO_2, the presence of acetic acid has a noticeable effect on the nature of corrosion damage to metal equipment. A detailed study of the role of acetic acid in carbon dioxide corrosion of carbon steel was carried out in [5]. Electrochemical measurements while maintaining a constant pH value of the medium have shown that additions of acetic acid significantly increase the limiting cathode current and slow down the anodic reaction at room temperature. The corrosion process is under kinetic control. At elevated temperatures, the effect of acetic acid is most pronounced and the corrosion process is controlled by mass transfer. No tendency to pitting corrosion has been identified. The authors believe that the undissociated form of acetic acid present at low pH is responsible for the increase in corrosion rates.

It is noted in [6, 7] that temperature, composition of the aqueous phase, the presence of CH_3COOH and mixing are the main factors influencing the increase in corrosion in hydrogen sulfide environments. Each of them, individually or together, to varying degrees, is capable of influencing the development of general and local hydrogen sulfide corrosion [8, 9]. Analysis shows that aqueous environments accompanying oil and gas fields have different mineralization and composition [10, 11]. The salinity and composition of the aquatic environment can have an important influence on corrosion in the presence of CO_2 and/or H_2S.

In [12, 13], the dependence of hydrogen sulfide corrosion on the H_2S content and the pH factor of the aquatic environment is noted, which is directly related to the possibility of either the formation of densely packed and more evenly distributed corrosion products on steel, or their absence.

According to [14], the presence of H_2S has a greater effect on corrosion than CO_2. In this case, the presence of chloride anions and the temperature of the environment have a stronger influence on the development of internal corrosion than CO_2. According to other data [15], when H_2S is added to a CO_2 environment, the corrosion rate can increase tens and even hundreds of times. The influence of CH_3COOH when introduced into an H_2S or CO_2 environment is significantly less. The authors of [16] in similar H_2S/CO_2 environments note an increase in general and local corrosion in the combined presence of two factors (CH_3COOH and elevated temperatures up to 55–85°C). Note that acidification with the addition of CH_3COOH will have a greater effect in carbon dioxide environments, dissolving or preventing the formation of an iron carbonate layer, than in hydrogen sulfide environments, where iron sulfide has much lower solubility.

According to [17], even small additions of H_2S (21 ppm) to the CO_2 environment are sufficient for the corrosion mechanism to change from carbon dioxide to hydrogen sulfide one. This leads to a change in the composition of corrosion products and only mackinawite

is formed on the steel (without traces of siderite). Due to its small thickness, the FeS film formed on steel is unable to act as a barrier to hydrogen sulfide corrosion [17].

Corrosion products (in the form of iron sulfides) begin to form on steel immediately after contact with an H_2S-containing aqueous environment. This is confirmed by visual observation of steel samples during the experiment. It should be noted that the composition, structure, thickness and durability of hydrogen sulfide corrosion products will be influenced by the above-mentioned main corrosive environmental factors (mineral composition and pH factor of water, temperature, H_2S content, *etc.*). The rate of hydrogen sulfide corrosion will depend on the properties of the film of corrosion products formed on the steel [18].

The morphology of iron sulfides (FeS) is quite different [19, 20]. Each form of FeS has its own conditions or sequence of formation that affect its properties and stability as hydrogen sulfide corrosion products on steel surfaces. Corrosive conditions have different effects on the shape, composition and properties of the resulting FeS deposits.

A comparative analysis showed differences in the morphology of corrosion products obtained from different aqueous solutions under hydrogen sulfide conditions [20]. The film of corrosion products formed in a 5% NaCl solution (in the presence/absence of CH_3COOH) was very compact and dense. In the model water under the same conditions, the FeS layer turned out to be very loose. At the same time, the authors of [21] found that at a higher H_2S content (2500 mg/L), a dense black deposit forms on the steel surface, and at a lower content (50 mg/L H_2S), a loose film of iron sulfides forms.

In mixed CO_2/H_2S environments, iron sulfide can form either independently or together with iron carbonate [22]. The composition of corrosion products will depend on the CO_2/H_2S ratio and other associated aggressive factors. The study [23] notes that when H_2S/CO_2 is combined in the system, mackinawite is predominantly formed, especially when the H_2S content prevails over CO_2 one. For the simultaneous formation of FeS and $FeCO_3$, a large amount of Fe^{2+} cations dissolved in the aqueous medium is required.

Another analysis of hydrogen sulfide corrosion products by X-ray diffraction in the combined presence of H_2S/CO_2 showed [24] that the content of crystalline compounds on the steels studied was 30–100% (the rest is X-ray amorphous substances). Of these crystalline compounds, the contents of mackinawite and siderite were 11–86% and 14–9%, respectively. Moreover, the concentration of $FeCO_3$ increased with a decrease in the proportion of FeS. This confirms that both corrosion products can be present together in the deposits. As the authors note [24], to isolate the surface of steels during hydrogen sulfide corrosion, it is important that the film of corrosion products be densely packed, which is more achievable in the presence of well-formed crystalline compounds. The presence of X-ray amorphous substances will loosen corrosive products, making them more porous, less protective and insufficiently effective in aggressive operating conditions.

According to [25], in an acidic environment with the presence of CH_3COOH, the primary layer of corrosion products forms faster than in a neutral environment. However, the growth rate of the outer layer of deposits in an acidic aqueous solution may be less than

in a neutral one. This may be one of the reasons why the corrosion rate will be higher in an acidic environment than in a neutral one. At the same time, the authors of [26] found that acidification of the environment with the addition of CH_3COOH leads to a change in the composition of corrosion products and is the cause of the formation, in addition to the tetragonal (mackinawite), also of the cubic form of FeS. The formation of deposits with different crystal structures and different FeS facets will lead to the formation of a less cohesive and monolithic film, reducing its barrier (protective) potential. Calculations using data on the composition of hydrogen sulfide corrosion products obtained by X-ray diffraction showed [26] that the addition of CH_3COOH does not affect the size of the faces of mackinawite crystals. However, one of the main indicators in the diffraction patterns, the half-width of the diffraction lines (β), in the medium without CH_3COOH coincides with its reference value for mackinawite ($\beta = 0.1697$), while it is different in mackinawite formed in an aqueous medium acidified with acetic acid ($\beta = 0.1719$). This may indicate defects in the FeS crystal lattice in the form of microstresses, isomorphism, etc. and the corresponding decrease in the protective properties of such corrosion products [26, 27]. Studies of hydrogen sulfide corrosion show that mackinawite is not capable of providing a protective effect, especially under dynamic test conditions, due to its low adhesion to the steel surface and the possibility of being carried away by the flow of the medium [27].

The reason for the insufficient effectiveness of inhibitor protection and increased pitting corrosion in hydrogen sulfide conditions may be either an insufficient concentration of a corrosion inhibitor (to form a uniform layer on steel) or a low rate of adsorption on the metal surface (compared to reactive FeS). The authors of [28] reported the possibility of competitive adsorption between iron sulfide and the corrosion inhibitor studied on a steel surface, which could undermine the integrity of the inhibitor film. At the same time, it is known that in hydrogen sulfide environments, the presence of sulfide or hydrosulfide anions on the surface of the steel can promote adsorption of some corrosion inhibitors.

Recently, mixtures of various compounds dissolved in specially selected mixed solvents are often used as inhibitors. Their composition, as a rule, contains imidazolines, polyamines, quaternary salts, alcohols, *etc*.

The purpose of this work is to study the influence of the composition of model stratum waters containing acetic acid and saturated with H_2S and CO_2 on the corrosion of St3 steel and the protective effect of the inhibitory composition provided by Gazprom VNIIGAZ LLC.

Experimental

Gravimetric and impedance measurements were carried out on samples of St3 steel with composition, mass. %: C – 0.2; Mn – 0.5; Si – 0.15; P – 0.04; S – 0.05; Cr – 0.30; Ni – 0.20; Cu – 0.20; Fe – 98.36.

Model stratum waters with the following compositions were used:

- MW1, g/L: NaCl – 30, CH_3COOH – 0.25;

- MW2, g/L: Na_2SO_4 – 1.4703, $CaCl_2 \cdot 2H_2O$ – 21.1974, $MgCl_2$ – 1.6393, NaCl – 73.1014, CH_3COOH – 0.25.

Hydrogen sulfide (400 mg/l) and carbon dioxide (1 excess atmosphere) were introduced into these media. Hydrogen sulfide was obtained directly in the working solution by introducing calculated amounts of Na_2S and HCl with iodometric concentration control. CO_2 was pumped from a high pressure cylinder.

The values of total salinity of waters MW1 and MW2 selected for testing are in the range typical for most oil and gas facilities.

The inhibitory composition is a solution of nitrogen-containing compounds (polyamines) in a mixture of organic solvents.

Gravimetric corrosion tests at room temperature and 80°C for 24 hours and 1 hour, respectively, were carried out under static conditions. A number of experiments were performed in a two-phase system "hydrocarbon phase – electrolyte solution (1:9)" under dynamic conditions (~240 rpm). Diesel fuel was used as the hydrocarbon phase. In this case, the duration of the experiment was 6 hours. The corrosion test procedure is described [29].

The protective effect of the inhibitory composition (25–200 mg/L) is calculated according to gravimetric corrosion tests and impedance measurements using the formulas:

$$Z,\% = \frac{\left(K_0 - K_{\text{Inh}}\right)}{K_0} \cdot 100 \quad (1)$$

$$Z,\% = \frac{\left(R_{\text{p,Inh}} - R_{\text{p,0}}\right)}{R_{\text{p,Inh}}} \cdot 100 \quad (2)$$

where K_0 and K_{Inh} are the corrosion rate in the absence and presence of an inhibitor in solution, respectively; $R_{\text{p,Inh}}$ and $R_{\text{p,0}}$ are the values of polarization resistance in a medium with and without an inhibitor, respectively, calculated on the basis of an equivalent impedance circuit. Impedance measurements were carried out according to [29]. Polarization resistance is calculated by the formula:

$$R_{\text{p}} = \frac{\left[R_1 \cdot \left(R_2 + R_{\text{D}}\right)\right]}{\left(R_1 + R_2 + R_{\text{D}}\right)}, \quad (3)$$

where R_1 and R_2 are the charge transfer resistances in the anodic and cathodic reactions, respectively, and R_{D} is the mass transfer resistance.

Before the experiments, the working electrodes were ground to class 6 cleanliness and degreased with acetone.

Results and Discussion

Table 1 shows the results of the gravimetric determination of the corrosion rate of St3 steel and the protective effect of the inhibitory composition in daily experiments in MW1 and

MW2 environments saturated with H_2S (400 mg/L). In background solutions, the corrosion rate in medium MW1 is higher than in medium MW2, and in the presence of an inhibitory composition, on the contrary, it is lower, with the exception of the solution with c_{Inh}=100 mg/L. This is reflected in the smaller protective effect of the inhibitor in the MW2 environment.

Table 1. Corrosion rate of St3 steel and the protective effect of the inhibitor in MW1 and MW2 media saturated with H_2S (400 mg/L) at room temperature.

c_{Inh}, mg/L	*K*, g/(m²·h)		*Z*, %	
	MW1+H_2S	MW2+H_2S	MW1+H_2S	MW2+H_2S
0	0.4150	0.3087	–	–
25	0.2639	0.2672	36	15
50	0.1750	0.1876	59	39
100	0.1635	0.1555	61	50
200	0.0983	0.1336	76	57

The presence of carbon dioxide in the MW1 and MW2 environments along with H_2S helps to increase the protective effectiveness of the inhibitory composition (Table 2). At its concentration of 200 mg/L, the value of Z=90%.

Table 2. Corrosion rate of St3 steel and the protective effect of the inhibitor in MW1 and MW2 media saturated with CO_2 (1 atm.)+H_2S (400 mg/L) at room temperature.

c_{Inh}, mg/L	*K*, g/(m²·h)		*Z*, %	
	MW1	MW2	MW1	MW2
0	0.6480	0.5719	–	–
25	0.4288	0.1281	34	78
50	0.2194	0.1181	66	79
100	0.1319	0.1009	80	82
200	0.0654	0.0591	90	90

In background solutions with CO_2 and H_2S, the corrosion rate is higher than in background solutions with H_2S, and in the presence of an inhibitor in the MW2 environment, on the contrary, it is lower, and in the MW1 environment it is lower only at c_{Inh}=100 and 200 mg/L. In the presence of CO_2 and H_2S, the corrosion rate in MW2 is lower than in MW1, both in the background solution and at all the inhibitor concentrations, and the Z values are close to each other at the two highest concentrations.

At 80°C, the protective efficiency of the inhibitor in the presence of H_2S is close to that at room temperature, both in MW1 and MW2 (Table 3).

Table 3. Corrosion rate of St3 steel and the protective effect of the inhibitor in MW1 and MW2 media saturated with H_2S (400 mg/L) at 80°C.

c_{Inh}, mg/L	*K*, g/(m²·h)		*Z*, %	
	MW1	MW2	MW1	MW2
0	10.4566	6.4324	–	–
25	5.9601	4.9590	43	23
50	5.6845	4.4554	46	31
100	3.9994	3.6671	62	43
200	3.1507	2.5986	70	60

The corrosion rate of steel in both background and inhibited solutions is higher in MW1 than in MW2.

In simulated stratum waters containing CO_2+H_2S, the protective effectiveness of the inhibitory composition at 80°C is higher than in the presence of H_2S (Table 4), as was also observed at room temperature. At c_{Inh}=200 mg/L, the *Z* values are close to 90%.

Table 4. Corrosion rate of St3 steel and the protective effect of the inhibitor in MW1 and MW2 media saturated with CO_2 (1 atm.)+H_2S (400 mg/L) at 80°C.

c_{Inh}, mg/L	*K*, g/(m²·h)		*Z*, %	
	MW1	MW2	MW1	MW2
0	11.9295	9.2955	–	–
25	5.7746	3.9408	52	70
50	4.5242	3.2692	62	75
100	3.9884	2.3414	67	82
200	1.4105	1.2993	88	90

In background solutions MW1 and MW2 with H_2S and CO_2, the corrosion rate at 80° is higher than in the presence of H_2S, and in an inhibited environment, on the contrary, it is lower. It should also be noted that in the presence of both corrosion stimulants, the corrosion rate in MW1 environments is higher than in MW2 ones.

In a two-phase system in the presence of hydrogen sulfide under dynamic conditions, the corrosion rate in MW1 is higher than in MW2 both in background and inhibited solutions (Table 5). It should be noted that the corrosion rate is higher compared to static conditions.

The protective effect of the inhibitor is significantly higher than in all other cases and is characterized by similar values in both environments. This is obviously due to the hydrophobization of the steel surface by the hydrocarbon component, since it wets the electrode surface better than an aqueous medium.

Table 5. Corrosion rate of St3 steel and the protective effect of the inhibitor in MW1 and MW2 media saturated with H_2S (400 mg/L) with stirring and in the presence of a hydrocarbon phase.

c_{Inh}, mg/L	*K*, g/(m²·h)		*Z*, %	
	MW1	MW2	MW1	MW2
0	4.7621	3.2402	–	–
25	1.1418	0.7700	76	76
50	1.0434	0.5802	78	82
100	0.3714	0.1852	92	94
200	0.0710	0.1336	98	96

A significant acceleration of hydrogen sulfide corrosion during the transition from static to dynamic test conditions is noted in [30–32]. This is due to the fact that the dynamic factor of the test conditions promotes both the removal of corrosion products from the surface of the steel, and the delivery of aggressive components to it to continue the corrosion process.

According to the authors [30], in an H_2S-containing two-phase environment (aqueous solutions with a mineralization of 100–200 g/L), the corrosion rate reached 0.725–0.935 mm/year at 20–30°C, increasing 4–6 times when the temperature increased to 80°C.

With the simultaneous presence of H_2S and CO_2 in two-phase systems with MW1 and MW2, approximately the same protective efficiency of the inhibitor is observed as in single-phase systems under static conditions, although lower than in two-phase systems in the presence of only H_2S (Table 6).

Analysis of the data presented indicates that the corrosion rate of steel in MW1 environments is higher than in MW2 environments in almost all cases considered. The MW2 environment is more saturated with salts than MW1. To a first approximation, it can be assumed that the reason for the lower aggressiveness is the higher viscosity of MW2, which leads to a slower diffusion of medium components to the electrode surface and a slower removal of corrosion products. And besides, the higher the concentration of salts in the solution, the lower the solubility of oxygen.

In uninhibited solutions, slight pitting is observed on the surface of the samples, and in environments with CO_2 to a lesser extent than in the presence of hydrogen sulfide alone. The presence of an inhibitor in the solution contributes to the absence of pitting.

Table 6. Corrosion rate of St3 steel and the protective effect of the inhibitor in MW1 and MW2 media saturated with CO_2 (1 atm.)+H_2S (400 mg/L) with stirring and in the presence of a hydrocarbon phase.

c_{Inh}, mg/L	*K*, g/(m²·h)		*Z*, %	
	MW1	MW2	MW1	MW2
0	5.1732	3.3697	–	–
25	3.0576	0.7081	41	79
50	2.0935	0.6631	60	80
100	1.0339	0.6524	80	81
200	0.4012	0.3686	92	89

The higher protective effectiveness of the inhibitor in the simultaneous presence of H_2S and CO_2 in solution than in the presence of H_2S alone, observed both at room temperature and at 80°C, may be associated with the inhibitory properties of CO_2, manifested in the acidic environment created by acetic acid. In a solution saturated with CO_2, carbonic acid is formed by the reaction:

$$CO_2 + H_2O \leftrightarrow H_2CO_3 \quad (4)$$

However, its amount is insignificant, according to the ratio $[CO_2]/[H_2CO_3]=296$ [3], and the dissociation $H_2CO_3 \leftrightarrow H^+ + HCO_3^-$ is suppressed in the presence of stronger acetic acid (K_{dis} (CH_3COOH)$=1.8\cdot10^{-5}$; K_{1dis} (H_2CO_3)$=4\cdot10^{-7}$; K_{2dis} (H_2CO_3)$=5.6\cdot10^{-11}$). Moreover, the dissociation of hydrosulfide acid H_2S is suppressed, since its dissociation constant in the first step is an order of magnitude lower than that of carbonic acid (K_{1dis} (H_2S) $= 8.9\cdot10^{-8}$). Still Ya.M. Kolotyrkin showed in [33] that saturation of a sulfuric acid solution with carbon dioxide slows down the anodic reaction on nickel. A similar phenomenon was noted by G.G. Uhlig for austenitic chromium-nickel steel (18% Cr, 8% Ni), the corrosion rate of which in a 6.3 N HCl solution decreases 470 times when CO_2 is introduced into the solution [34]. The observed phenomena are explained by the authors by the adsorption of CO_2 on the electrode. A similar inhibitory effect of CO_2 was observed in [35] on St3 steel in weakly acidic (0.005 N, 0.01 N) HCl solutions, and the higher the acidity of the medium, the stronger the inhibition, *i.e.* clearly the effect was exerted by CO_2 molecules, and not by HCO_3^- or CO_3^{2-} ions.

However, it is not clear why the retarding effect of CO_2 is not manifested in the background solutions MW1 and MW2. To a first approximation, it can be assumed that the adsorption of acetic acid and acetate ions on the electrode surface prevents the adsorption of CO_2. And in inhibited media, the adsorption of the components of the inhibitory composition prevents the adsorption of CH_3COOH molecules and anions, but does not affect the adsorption of CO_2.

In the presence of a hydrocarbon phase that hydrophobizes the metal surface, the adsorption of CO_2 on the surface is obviously hindered by the hydrophobic film and therefore the protective effect does not increase compared to media containing H_2S.

To resolve the issue of the mechanism of the inhibitory action, the apparent activation energy E_a of the corrosion process in the studied solutions in the absence and presence of an inhibitor was calculated using the Arrhenius equation:

$$\ln\left(\frac{K_2}{K_1}\right)=\left[\frac{E_a\left(T_2-T_1\right)}{RT_1\cdot T_2}\right], \quad (5)$$

where K_1 and K_2 are the corrosion rates of steel at temperatures of 293 K and 353 K, respectively, T_1=293 K, T_2=353 K. The E_a values obtained are given in Table 7, from which it follows that in environments inhibited the activation energy of the process differs from its value in background solutions, although only slightly. If these values coincide, it could be argued that there is a blocking mechanism of the inhibitor. The small difference observed allows us to assume a mixed mechanism: blocking along with energy one.

Table 7. The values of the apparent (effective) activation energy of the steel corrosion process in media under study.

Medium	$E_{a,eff.}$, kJ/mol at c_{Inh}, mg/L				
	0	25	50	100	200
MW1+H_2S	46.2	44.6	49.9	45.8	49.7
MW1+H_2S+CO_2	41.7	37.2	43.3	48.8	44.0
MW2+H_2S	43.5	41.8	45.4	45.4	42.5
MW2+H_2S+CO_2	40.0	49.1	47.6	45.0	44.3

Impedance studies confirm the protective effectiveness of the studied inhibitory composition. As an example, consider the corresponding results for MW2. Figure 1 shows the Nyquist diagram for a steel electrode in an MW2+H_2S environment.

Table 8 presents the numerical values of the elements of an equivalent circuit simulating a steel electrode in the solution under study [29].

The value of charge transfer resistance in the anodic process R_1 increases with the introduction of an inhibitor into the solution and an increase in its concentration, indicating a slowdown in the anodic reaction. The values of charge transfer resistance in the cathodic process R_2 change slightly. The capacitance values of the electrical double layer C_{dl} decrease with the introduction of an inhibitor and an increase in its concentration. This indicates the adsorption of the inhibitor on the surface of the steel electrode. The resistance of diffusion mass transfer R_D significantly exceeds the resistance of charge transfer in the cathodic process R_2. This indicates the reduction of the depolarizer with a predominance of diffusion

restrictions. The values of the protective effect, calculated according to the polarization resistance R_p, increase with an increase in the inhibitor concentration, that is consistent with the results of gravimetric measurements.

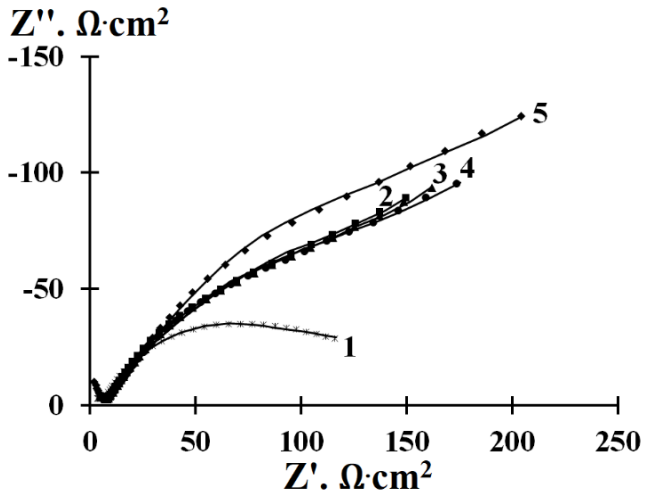

Figure 1. Nyquist diagram of a steel electrode in MW2 media saturated with H_2S (400 mg/L) at E_{corr} in the absence (1) and in the presence of inhibitory composition, mg/L: 2 – 25; 3 – 50; 4 – 100; 5 – 200. The dots correspond to the experimental data, whereas the solid lines correspond to the impedance spectra fitted using the equivalent circuit.

Table 8. Numerical values of elements of the equivalent circuit at E_{corr} of the steel electrode in MW2 media saturated with H_2S (400 mg/L) without and with tested concentrations of the inhibitory composition.

Element	Concentration of inhibitory composition, mg/L				
	Background	**25**	**50**	**100**	**200**
R_s, Ω·cm²	0.8	3.3	3.4	3.6	2.2
C_a, μF/cm²	179.5	185.8	117.2	112.6	11.7
R_1, Ω·cm²	138.6	430.8	432.2	492.5	537.5
C_{dl}, μF/cm²	26.9	19.0	11.8	10.1	10.1
R_2, Ω·cm²	5.1	4.2	4.8	3.6	8.3
R_a, Ω·cm²	44.0	18.6	24.7	32.2	30.0
R_D, Ω·cm²	896	951	1039	1124	1398
τ_d, s	8.4	15.9	15.1	19.4	7.1
p_d	0.6	0.5	0.5	0.5	0.6
s, %	2.9	4.0	4.3	3.3	3.9
R_p, Ω·cm²	120.1	296.9	305.6	342.8	388.9
Z, %	–	59	61	65	69

The C_{dl} values obtained make it possible to calculate the steel surface coverage with the components of the inhibitory composition according to formula (6):

$$\Theta = \frac{C_0 - C}{C_0 - C_1}, \quad (6)$$

where C_0, C and C_1 are the capacitances of the electric double layer in the solution without addition of inhibitory composition, with that and with the maximum coverage of the electrode surface with the adsorbed particles, respectively. The value of C_1 is calculated graphically on the basis of the rectilinear dependence $C_{dl} = C_{dl}(1/c_{inh})$ and is equal to the segment cut off on the y-axis (Figure 2). In the MW2 environment, saturated with H_2S (400 mg/L), the value of C_1 is 7.75 μF/cm^2. The calculated values of Θ are given in Table 9.

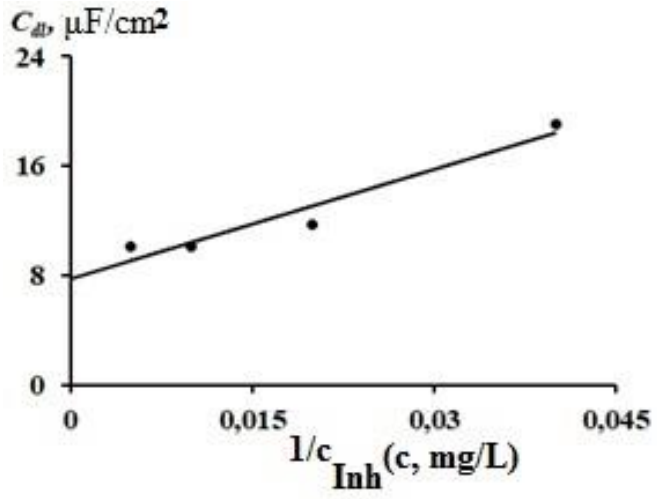

Figure 2. The dependence of C_{dl} on $1/c_{Inh}$ in MW2 media saturated with H_2S (400 mg/L).

Table 9. The values of the electrode surface coverage with the inhibitory composition in MW2 media saturated with H_2S (400 mg/L).

c_{Inh}, mg/L	25	50	100	200
Θ	0.41	0.79	0.87	0.88

To select an isotherm corresponding to the data given in Table 9, it was checked their correspondence to the Temkin isotherm $Bc = \exp(f \cdot \Theta)$, the Frumkin isotherm $Bc = [\Theta/(1-\Theta)]\exp(-2a\Theta)$, and the Langmuir isotherm $c/\Theta = 1/B + c$, where f is the factor of the energy inhomogeneity of the surface, B is the constant of adsorption equilibrium, a is the attraction constant characterizing the interaction between adsorbed particles, c is inhibitor concentration. For this, the graphic dependences of Θ *vs.* (ln$c$), ln[$c(1-\Theta)/\Theta$] *vs.* Θ and c/Θ *vs.* c corresponding to the Temkin, Frumkin and Langmuir isotherms, respectively, were considered (Figure 3).

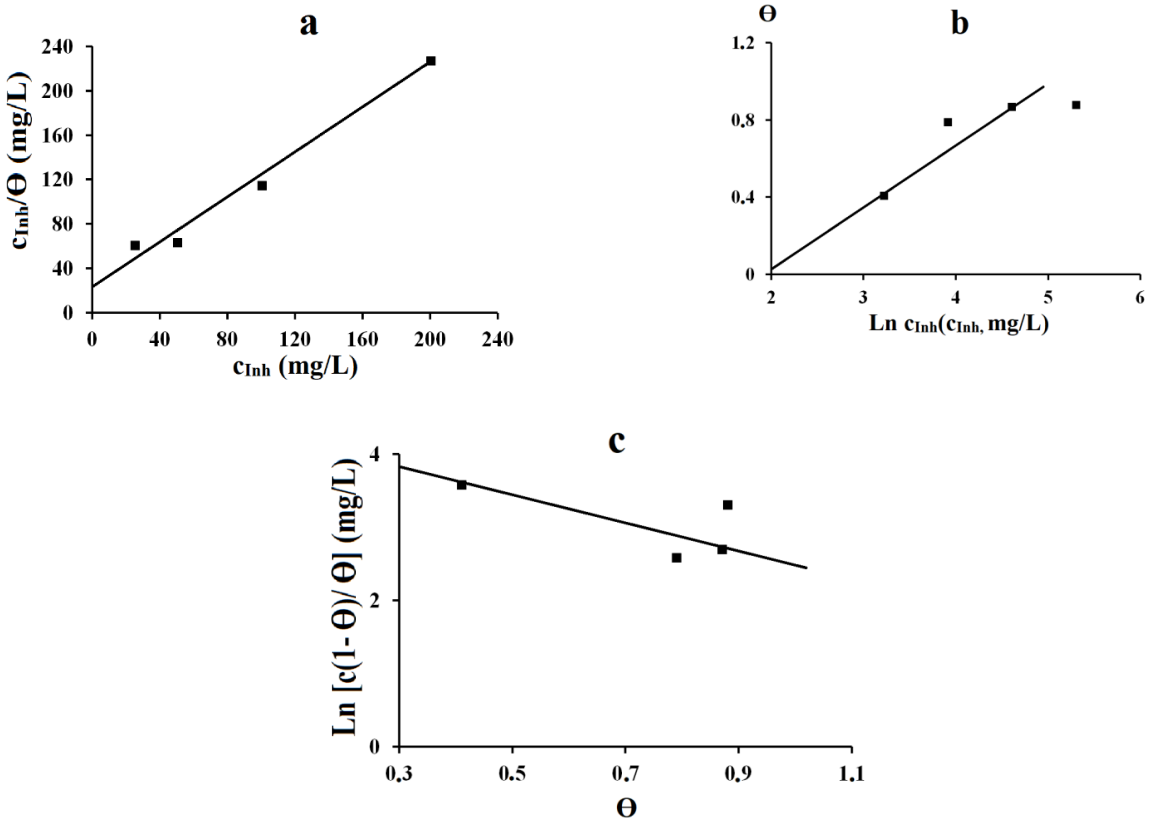

Figure 3. Adsorption isotherms for St3 steel in MW2+H_2S (400 mg/L).

It turned out that the best fitting of the data to the linear dependence corresponds to the Langmuir isotherm (Figure 3a). The segment cut off on the vertical axis of Figure 3a makes it possible to calculate the adsorption equilibrium constant *B*. The value of *B* is 0.038 L/mg. The value of *B* enables us to calculate the value of free adsorption energy according to the formula (7):

$$-\Delta G_{ads}^{0} = RT \ln\left(B \cdot 10^{6}\right), \quad (7)$$

where 10^6 is the concentration of water in the solution, mg/L. The value $-\Delta G_{ads}^{0}$ at a temperature of 298 K is 26 kJ/mol. It can be assumed that the adsorption of the components of the inhibitory composition is due to physical forces with a certain amount of chemisorption.

Figure 4 shows hodographs on the Nyquist diagram for a steel electrode in an MW2+H_2S+CO_2 environment in the absence and presence of additives of an inhibitory composition. They are arcs, the diameter of which increases with increasing concentration of the inhibitory composition. This indicates an increase in the overall resistance in the system and, consequently, a decrease in the corrosion rate.

The numerical values of the elements of the equivalent circuit (Table 10) indicate that the charge transfer resistance in the anodic process R_1 increases with the introduction of an

inhibitor and an increase in its concentration, which indicates inhibition of the anodic process. The values of R_2 and C_{dl} change similarly to their change in a solution with H_2S.

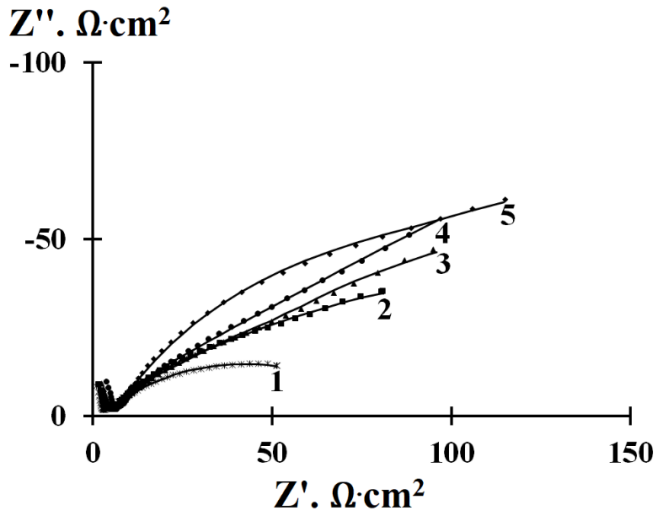

Figure 4. Nyquist diagram of a steel electrode in MW2 media saturated with CO_2 (1 atm)+ H_2S (400 mg/L) at E_{corr} in the absence (1) and in the presence of inhibitory composition, mg/L: 2 – 25; 3 – 50; 4 – 100; 5 – 200. The dots correspond to the experimental data, whereas the solid lines correspond to the impedance spectra fitted using the equivalent circuit.

Table 10. Numerical values of elements of the equivalent circuit at E_{corr} of the steel electrode in MW2 media saturated with CO_2 (1 atm.)+H_2S (400 mg/L) without and with tested concentrations of the inhibitory composition.

Element	Concentration of inhibitory composition, mg/L				
	Background	**25**	**50**	**100**	**200**
R_s, Ω·cm²	1.5	2.2	2.4	3.9	1.6
C_a, μF/cm²	39.0	213.0	160.0	189.8	240.5
R_1, Ω·cm²	62.8	111.0	340.1	381.1	426.1
C_{dl}, μF/cm²	36.0	22.6	20.3	20.0	12.9
R_2, Ω·cm²	3.8	5.7	2.8	3.4	5.1
R_a, Ω·cm²	9.7	13.1	19.4	11.4	15.6
R_D, Ω·cm²	289.7	304.7	344.6	468.3	886.4
τ_d, s	8.9	6.4	34.8	31.2	9.8
p_d	0.5	0.5	0.4	0.4	0.6
s, %	3.2	3.2	3.9	4.6	3.4
R_p, Ω·cm²	51.8	81.8	171.9	210.8	288.3
Z, %	–	37	70	75	82

The protective effectiveness of the inhibitor, calculated from the polarization resistance R_p, exceeds the corresponding values in the MW2+H_2S medium and is consistent with the Z values determined in gravimetric tests.

Using data on the reduction in the capacity of the double electric layer C_{dl}, the steel surface coverage with the components of the inhibitory composition was calculated according to formula (6) and the method described above for the MW2+H_2S solution. The corresponding Θ values are given in Table 11.

Table 11. The values of the electrode surface coverage with the inhibitory composition in MW2 media saturated with CO_2 (1 atm)+H_2S (400 mg/L).

c_{Inh}, mg/L	25	50	100	200
Θ	0.53	0.62	0.63	0.91

It turned out that the obtained Θ values correspond to the Langmuir isotherm with the adsorption equilibrium constant B coinciding with that for the MW2+H_2S medium. Accordingly, the value of the free energy of adsorption $-\Delta G^0_{ads}$ has the same value, indicating the physical nature of the adsorption of the components of the inhibitory composition with a certain amount of chemisorption.

Conclusion

The corrosion and protective effectiveness of an inhibitory composition representing a solution of nitrogen-containing compounds (polyamines) in a mixture of organic solvents were studied in relation to St3 steel in simulated stratum waters MW1 and MW2, differing in the degree of mineralization, saturated with H_2S and CO_2 and containing 0.25 mg/L CH_3COOH.

Gravimetric studies under static conditions at room temperature and 80°C showed that the corrosion rate of steel is lower in more mineralized environments of MW2 than in MW1. The same picture is observed in two-phase systems containing 10% hydrocarbon phase under dynamic conditions.

The protective effectiveness Z of the inhibitory composition in the presence of H_2S in solution is higher in MW1 media, and in the presence of H_2S and CO_2, on the contrary, in MW2 at room temperature and 80°C.

The presence of H_2S and CO_2 contributes to a higher protective effectiveness of the inhibitory composition in both stratum waters (Z = 90%) compared to the presence of only H_2S (Z = 60–70%) both at room temperature and at 80°. This is confirmed by impedance measurements. Under dynamic conditions in the presence of a hydrocarbon phase, the Z value exceeds 90%.

The impedance spectroscopy method made it possible to determine the adsorption of the components of the inhibitory composition, the adsorption isotherm and calculate the free energy of adsorption equal to 26 kJ/mol.

The morphology of the forms and composition of iron sulfides (density/looseness, absence/presence of pores), as well as thickness, can affect the barrier properties of the resulting corrosion products under conditions of hydrogen sulfide corrosion.

Acknowledgment

The results were obtained using the equipment of the Center for Collective Use of Scientific Equipment of TSU named after G.R. Derzhavin. The study was carried out as part of the development program of TSU named after G.R. Derzhavin "Priority-2030".

References

1. R.K. Vagapov, Corrosion Destruction of Steel Equipment and Pipelines at Gas Field Facilities in the Presence of Aggressive Components, *Steel in Translation*, 2023, **53**, no. 1, 5–10. doi: 10.3103/S0967091223010138
2. B. Obot, M.M. Solomon, S.A. Umoren, R. Suleiman, M. Elanany, N.M. Alanazi and A.A. Sorour, Progress in the development of sour corrosion inhibitors: Past, present, and future perspectives, *J. Ind. Eng. Chem*., 2019, **79**, 1–18. doi: 10.1016/j.jiec.2019.06.046
3. V.I. Vigdorovich and L.E. Tsygankova, *Inhibition of hydrogen sulfide and carbon dioxide corrosion of metals. Universalism of inhibitors*, Monograph, 2011, Moscow, CARTEC, 244 (in Russian).
4. A.N. Markin and R.E. Nizamov, *CO_2 corrosion of oil field equipment*, Moscow, JSC "VNIIOENG", 2003, 187 (in Russian).
5. K.S. George and S. Nešic, Investigation of carbon dioxide corrosion of mild steel in the presence of acetic acid – Part 1. Basic mechanisms, *Corrosion*, 2007, **63**, no. 2, 178–186. doi: 10.5006/1.3278342
6. H. Ma, X. Cheng, G. Li, Sh. Chen, Zh. Quan, Sh. Zhao and L. Niu, The influence of hydrogen sulfide on corrosion of iron under different conditions, *Corros. Sci*., 2000, **42**, no. 10, 1669–1683. doi: 10.1016/S0010-938X(00)00003-2
7. F. Pessu, R. Barker and A. Neville, Pitting and Uniform Corrosion of X65 Carbon Steel in Sour Corrosion Environments: The Influence of CO_2, H_2S, and Temperature, *Corrosion*, 2017, **73**, no. 9, 1168–1183. doi: 10.5006/2454
8. M. Qin, K. Liao, G. He, Q. Zou, Sh. Zhao and Sh. Zhang, Corrosion mechanism of X65 steel exposed to H_2S/CO_2 brine and H_2S/CO_2 vapor corrosion environments, *J. Natur. Gas Sci. Eng*., 2022, **106**, 104774. doi: 10.1016/j.jngse.2022.104774
9. F. Pessu, Y. Hua, R. Barker and A. Neville, A Study of the Pitting and Uniform Corrosion Characteristics of X65 Carbon Steel in Different H_2S-CO_2-Containing Environments, *Corrosion*, 2018, **74**, no. 8, 886–902. doi: 10.5006/2537
10. I.I. Baydin, A.V. Kovalenko, N.V. Gumerova and An.V. Kovalenko, Analysis of the dynamics of reservoir water introduction in the gas reservoir on the decline of gas production, *Izvestiâ vysših učebnyh zavedenij. Neft' i gaz* (*Oil and Gas)*, 2018, **6**, 41–44 (in Russian). doi: 10.31660/0445-0108-2018-6-41-44

11. A.V. Koshelev, G.S. Lie and M.A. Katayeva, Operative hydrochemical control over the watering out of the formation waters of the development sites of the Urengoyskoye oil and gas condensate field, *Vesti Gazovoy Nauki*, 2014, **19**, no. 3, 106–115 (in Russian).
12. N.M. Alanazi and A.A. Al-Enezi, The Effect of the Partial Pressure of H_2S and CO_2 on the Permeation of Hydrogen in Carbon Steel by Using Pressure Buildup Techniques, *Corrosion*, 2019, **75**, no. 10, 1207–1215. doi: 10.5006/3128
13. J. Kittel, V. Smanio, M. Fregonese, L. Garnier and X. Lefebvre, Hydrogen induced cracking (HIC) testing of low alloy steel in sour environment: Impact of time of exposure on the extent of damage, *Corros. Sci*., 2010, **52**, no. 4, 1386–1392. doi: 10.1016/j.corsci.2009.11.044
14. P. Huan, F. Pan, L. Heng and S. Hechao, Corrosion sensitivity analysis of pipelines in CO_2 and H_2S coexisting environment in the South China Sea, *Corros. Rev*., 2022, **40**, no. 4, 355–368. doi: 10.1515/corrrev-2021-0052
15. M. Singer, B. Brown, A. Camacho and S. Nešić, Combined Effect of Carbon Dioxide, Hydrogen Sulfide, and Acetic Acid on Bottom-of-the-Line Corrosion, *Corrosion*, 2011, **67**, no. 1. doi: 10.5006/1.3543715
16. A. Talukdar and P.V. Rajaraman, Effect of acetic acid in CO_2-H_2S corrosion of carbon steel at elevated temperature, *Mater. Today: Proc*., 2022, **57**, no. 4, 1842–1845. doi: 10.1016/j.matpr.2022.01.036
17. S.C. Silva, A.B. Silva and J.A.C. Ponciano Gomes, Hydrogen embrittlement of API 5L X65 pipeline steel in CO_2 containing low H_2S concentration environment, *Eng. Failure Anal*., 2021, **120**, 105081. doi: 10.1016/j.engfailanal.2020.105081
18. Zh. Liu, Y. Wang, Y. Zhai, Y. Qiao, Ch. Zheng, D. Wang, X. Shi, H. Lu and Ch. Liu, Corrosion behavior of low alloy steel used for new pipeline exposed to H_2S-saturated solution, *Int. J. Hydrogen Energy*, 2022, **47**, no. 77, 33000–33013. doi: 10.1016/j.ijhydene.2022.07.203
19. F. Shi, L. Zhang, J. Yang, M. Lu, J. Ding and H. Li, Polymorphous FeS corrosion products of pipeline steel under highly sour conditions, *Corros. Sci*., 2016, **102**, 103–113. doi: 10.1016/j.corsci.2015.09.024
20. Sh. Zhen, L. Liu, Ch. Zhou, L. Chen and Ch. Chen, Effects of H_2S-containing Corrosive Media on the Crystal Structures of Corrosion Product Films Formed on L360NCS, *Int. J. Electrochem. Sci*., 2013, **8**, no. 1, 1434–1442. doi: 10.1016/S1452-3981(23)14109-5
21. E.S. Ivanov, M.L. Brodskii, Yu.V. Ryabov and A.Y. Timonin, Investigation of corrosion stability and trend to stress corrosion fracture of new tube steel 08XMFChA in hydrogen sulfide containing media of oil fields, *Theory and Practice of Corrosion Protection*, 2009, **53**, no. 3, 8–19 (in Russian).
22. S.J. Dong, G.S. Zhou, X.X. Li, S. Ouyang and H.F. An, Comparison of corrosion scales formed on KO80SS and N80 steels in CO_2/H_2S environment, *Corros. Eng., Sci. Technol*., 2011, **46**, no. 6, 692–696, doi: 10.1179/147842210X12692706339229

23. W. Sun, S. Nešić and S. Papavinasam, Kinetics of Corrosion Layer Formation. Part 2—Iron Sulfide and Mixed Iron Sulfide/Carbonate Layers in Carbon Dioxide/Hydrogen Sulfide Corrosion, *Corrosion*, 2008, **64**, no. 7, 586–599. doi: 10.5006/1.3278494
24. R.R. Kantyukov, D.N. Zapevalov and R.K. Vagapov, Assessment of the Effect of Operating Conditions on the Resistance of Steels Used in H_2S-Containing Environments at Hydrocarbon Production Facilities, *Metallurgist*, 2022, **65**, 1369–1380. doi: 10.1007/s11015-022-01284-4
25. C. Zhou, X. Chen, Z. Wang, S. Zheng, X. Li and L. Zhang, Effects of environmental conditions on hydrogen permeation of X52 pipeline steel exposed to high H_2S-containing solutions, *Corros. Sci*., 2014, **89**, 30–37. doi: 10.1016/j.corsci.2014.07.061
26. R.K. Vagapov, O.G. Mikhalkina, V.N. Lopatkin, K.A. Ibatullin and K.O. Strelnikova, Comparison of the aggressiveness of hydrogen sulfide media to steel in the vapor and water phases, *Vopr. Materialoved*., 2023, **115**, no. 3, 188–201 (in Russian). doi: 10.22349/1994-6716-2023-115-3-188-201
27. R.K. Vagapov, Study of Hydrogenation and Corrosion of Steel Equipment and Pipelines at the Production Facilities of H_2S-Containing Hydrocarbon Raw Materials, *Inorg. Mater.: Appl. Research*, 2022, **13**, no. 6, 1658–1665. doi: 10.1134/S2075113322060302
28. F. Pessu, R. Barker, F. Chang, T. Chen and A. Neville, Iron sulphide formation and interaction with corrosion inhibitor in H_2S-containing environments, *J. Pet. Sci. Eng*., 2021, **207**, 109152. doi: 10.1016/j.petrol.2021.109152
29. L.E. Tsygankova, A.E. Abramov, A.A. Uryadnikov, N.V. Shel, K.O. Strel'nikova, R.K. Vagapov, Inhibition of carbon steel corrosion in model stratum waters containing hydrogen sulfide, *Int. J. Corros. Scale Inhib*., 2023, **12**, no. 2, 410–423. doi: 10.17675/2305-6894-2023-12-2-2
30. R.K. Vagapov, K.A. Ibatullin and V.V. Yarkovoy, Simulation of the Modes of Medium Flow Movement through a Gas Pipeline during Corrosion Tests, *Zavodskaya laboratoriya. Diagnostika materialov (Ind. Lab. Materials Diagnostics)*, 2023, **88**, no. 10, 35–41 (in Russian). doi: 10.26896/1028-6861-2023-89-10-40-46
31. M. Qin, K. Liao, G. He, Y. Huang, M. Wang and Sh. Zhang, Main control factors and prediction model of flow-accelerated CO_2/H_2S synergistic corrosion for X65 steel, *Process Saf. Environ. Prot*., 2022, **160**, 749–762. doi: 10.1016/j.psep.2022.02.062
32. Sh. Zhang, Y. Li, B. Liu, L. Mou, Sh. Yu, Yu. Zhang and X. Yan, Understanding the synergistic effect of CO_2, H_2S and fluid flow towards carbon steel corrosion, *Vacuum*, 2022, **196**, 110790. doi: 10.1016/j.vacuum.2021.110790
33. Ya.M. Kolotyrkin, *Zashch. Met. (Prot. Met.)*, 1967, **3**, 131 (in Russian).
34. G.G. Uhlig and R.W. Revie, *Korroziya i bor'ba s nei. Vvedenie v korrozionnuyu nauku i tekhniku*, Leningrad, Khimiya, 1989, 456 (translation into Russian from: H.H. Uhlig and R.W. Revie, *Corrosion and corrosion control*, 3rd edn., Wiley-Interscience, New York, 1985).

35. S.E. Sinyutina, M.V. Loskutova, A.V. Boldyrev, E.K. Oshe, L.E. Tsygankova and V.I. Vigdorovich, Inhibition of steel corrosion in weakly acidic HCl solutions containing H_2S and CO_2, *Zhurnal prikladnoi khimii (J. Appl Chem*.) 1997, **70**, no. 3, 430–436 (in Russian).

♦ ♦ ♦